Sjl2p is specifically involved in early steps of endocytosis intimately linked to actin dynamics via the Ark1p/Prk1p kinases

Claudia Böttcher[a], Sidonie Wicky[a,1], Heinz Schwarz[b], Birgit Singer-Krüger[a,*]

[a] *University of Stuttgart, Institute for Biochemistry, Pfaffenwaldring 55, D-70569 Stuttgart, Germany*
[b] *Max-Planck Institute for Developmental Biology, D-72076 Tübingen, Germany*

Abstract Sjl2p is one of three yeast phosphoinositide 5′-phosphatases that belong to the conserved family of synaptojanins. Here, we show that Sjl2p is specifically associated with cortical actin patches which aggregate upon loss of the actin-regulating kinases Ark1p and Prk1p. The Sjl2p-containing clumps overlap with clathrin and early endocytic structures generated independently of NSF/Sec18p, but not with endosome- and *trans* Golgi network-derived membranes. Consistent with the finding that Sjl2p can bind to clathrin heavy chain in vitro, our results suggest that Sjl2p localizes to smooth endocytic vesicles that may be derived from clathrin-coated structures.
© 2005 Federation of European Biochemical Societies. Published by Elsevier B.V. All rights reserved.

1. Introduction

Phosphorylated derivatives of phosphatidylinositol, collectively called phosphoinositides (PIs), are short-lived lipids with signaling functions in diverse processes such as cell proliferation, actin cytoskeletal rearrangements, and vesicular traffic. Different PIs are concentrated in diverse subcellular compartments, with for example phosphatidylinositol 4-phosphate found on Golgi membranes, phosphatidylinositol 4,5-bisphosphate at the plasma membrane, and phosphatidylinositol 3-phosphate on early endosomes. The spatial segregation of the various PIs may be part of the mechanism by which the direction of membrane traffic is controlled [1]. PIs increase the affinity of membranes for peripheral membrane proteins with a role in the sorting of cargo molecules or in the docking and fusion of transport vesicles. Therefore, membrane traffic is likely regulated by the mechanisms that control the activity of the enzymes producing and consuming PIs.

The differential phosphorylation of PIs is mediated by specific kinases localized to distinct subcellular compartments. Conversely, a set of phosphatases and lipases regulates PI turnover, thereby controlling the distribution and duration of signaling events mediated by PI second messengers. Members of the highly conserved synaptojanin protein family are

PI 5′-phosphatases that have been demonstrated to fulfill essential roles in membrane trafficking and actin dynamics in all eukaryotes. Genetic disruption of mouse synaptojanin 1, the *Caenorhabditis elegans* ortholog unc-26, and the *Drosophila melanogaster* ortholog SynI leads to the accumulation of regularly spaced arrays of densely coated vesicles [2–4], suggesting that synaptojanin proteins function in clathrin uncoating or regulate cytoskeleton vesicle interactions during endocytosis, or both.

Yeast cells express three synaptojanin-like proteins, Sjl1p, Sjl2p, and Sjl3p, also designated as Inp51p, Inp52, Inp53p. Single Δ*sjl1*, Δ*sjl2*, Δ*sjl3* null mutants, and the Δ*sjl1* Δ*sjl3* double mutant are viable and display no obvious deficiencies. However, the Δ*sjl1* Δ*sjl2* and Δ*sjl2* Δ*sjl3* double mutants and temperature-sensitive *sjl2* alleles in a triple Δ*sjl1* Δ*sjl2* Δ*sjl3* background exhibit various phenotypes, including impaired cell growth, defects in receptor-mediated and fluid-phase endocytosis and actin organization, and abnormal morphologies of the plasma membrane with massive invaginations [5–8]. While these mutant studies emphasized the redundant functions of the three synaptojanin-like proteins, several lines of genetic evidence rather suggested specific roles for the three family members. Mutants in *PAN1*, *SAC6*, and in genes of the cell integrity pathway show genetic interactions with the deletion of *SJL1*, and mutations in *SJL3* in combination with a temperature-sensitive allele of clathrin heavy chain (*CHC1*) cause a defect in clathrin-dependent sorting at the *trans* Golgi network (TGN) [7,9–11].

In this work we present further evidence for a major and specific role of Sjl2p during early steps of endocytosis. We demonstrate a direct and unique connection between Sjl2p and actin dynamics via the actin-regulating kinases Ark1p and Prk1p and provide multiple evidence for an association of Sjl2p with primary endocytic vesicles. Our results corroborate the idea of distinct roles and subcellular localizations of the yeast synaptojanin-like proteins.

2. Materials and methods

2.1. Strains, media, and DNA manipulations

Yeast strains (Table 1) were grown in standard rich media (YPD) or synthetic media (SD) supplemented with the appropriate amino acids. *SJL1-HA*, *SJL2-HA*, *SJL3-HA*, *SJL2-GFP*, and *SJL2-13-Myc* specific fragments were generated by PCR using p3xHA-HIS5 (S. Munro, Cambridge, UK), pFA6a-3HA-kanMX6, pFA6a-13Myc-kanMX6, and pFA6a-GFP(S65T)-kanMX6 as templates [12] and were inserted at the chromosomal *SJL1*, *SJL2,* and *SJL3* loci by homologous recombination. The 3-HA-CLC1 integration cassette was generated

---

*Corresponding author. Fax: +49 711 685 4392.
E-mail address: Singer-Krueger@ibc.uni-stuttgart.de
(B. Singer-Krüger).

1 Present address: Sinsheimer Labs, University of California, Santa Cruz, CA, USA.

Table 1
Strains used Böttcher et al.

Yeast strain	Genotype	Source
BS64	*MATa his4 ura3 leu2 lys2 bar1-1*	[13]
BS1128	*MATα ura3 leu2 lys2 SJL2::3-HA-HIS5 (S. pombe) bar1-1*	This study
BS1175	*MATα ura3 leu2 SJL2:: 3-HA-HIS5 (S. pombe) sec7 bar1-1*	This study
BS1248	*MATa ura3 leu2 lys2 his4 SJL2::13-Myc-kan^r bar1-1*	This study
BS1271	*MATα ura3 leu2 SJL2::3-HA-HIS5 (S. pombe) Δark1::HIS3 Δprk1::LEU2*	This study
BS1373	*MATα ura3 leu2 lys2 Δark1::HIS3 Δprk1::LEU2 SJL1::3-HA-HIS5 (S. pombe)*	This study
BS1376	*MATa ura3 leu2 lys2 Δark1::HIS3 Δprk1::LEU2 SJL3::3-HA-kan^r*	This study
BS1417	BS1271 + pRS316-prk1-as3	This study
BS1430	BS1376 + pRS316-prk1-as3	This study
BS1446	*MATa ura3 leu2 lys2 Δark1::HIS3 Δprk1::LEU2 SJL2::GFP-kan^r* + pRS316-prk1-as3	This study
BS1516	*MATa ura3 leu2 his3 ade2 lys2 CLC1::3-HA-kan^r bar1-1*	This study
BS1521	*MATa ura3 leu2 his3 lys2 Δark1::HIS3 Δprk1::LEU2 CLC1::3-HA-kan^r* + pRS316-prk1-as3	This study
BS1569	*MATα ura3 leu2 lys2 Δark1::HIS3 Δprk1::LEU2 CLC1::3-HA-kan^r SJL2::13-Myc-kan^r* + pRS316-prk1-as3	This study
CB42	*MATα ura3 leu2 lys2 SJL1::3-HA-HIS5 (S. pombe) SJL2-13-Myc-kan^r SJL3::3-HA-kan^r bar1-1*	This study
CB84	*MATα ura3 leu2 lys2 his4 CLC1::3-HA-kan^r bar1-1*	This study
CB175	*MATa ura3 leu2 his4 SJL3::3-HA-kan^r sec7 bar1-1*	This study
DDY1885	*MATα ura3 his3 lys2 leu2 prk1Δ::LEU2 ark1Δ::HIS3*	David Drubin, Berkeley, CA

by subcloning the promotor of *CLC1* (bp −538 to −1) into the *Bgl*II and *Pac*I restriction sites of pFA6a-kanMX6-PGAL1-3HA [12]. This plasmid served as template to generate the *kan^r-pCLC1-3-HA-CLC1* cassette, which was integrated into the chromosomal *CLC1* locus. Diploid transformants were purified and correct integration was verified by PCR. Strains with multiple epitope-tagged genes were generated by crossing of haploids, sporulation of diploids, and selection of haploids by expression analysis.

DNA manipulations and yeast transformations were performed by standard techniques.

2.2. Immunofluorescence microscopy

Indirect immunofluorescence microscopy was performed as described [13]. Single stainings were performed with the monoclonal mouse α-HA antibody (16B12, Covance, 1:1000) and a Cy^3-conjugated goat anti-mouse Fab fragment (Jackson ImmunoResearch, 1:1000). For double stainings, dilutions for the primary antibodies were as follows: monoclonal mouse α-HA (16B12, Covance) 1:1000, monoclonal rat α-HA (clone 3F10, Roche) 1:50, monoclonal mouse α-Pep12p (Molecular Probes) 1:100, affinity purified rabbit α-Ypt51p [13] 1:50, rabbit α-c-Myc (Santa-Cruz Biotechnology) 1:150, and mouse α-c-Myc (Oncogene) 1:100. All secondary antibodies were affinity purified and used at a dilution of 1:1000; Alexa^{594}-conjugated goat anti-mouse IgG; Alexa^{488}-conjugated goat anti-rat IgG; Alexa^{488}-conjugated goat anti-rabbit IgG (Molecular Probes). GFP-Act1p was directly observed with appropriate filter sets.

FM4-64 labelling was performed essentially as described [14]. Internalization was carried out for 10 min at 25 °C in the presence of DMSO or 0.04 mM 1NA-PP1. Cells were harvested, resuspended in fresh SD medium with 10 mM NaF, 10 mM NaN$_3$, and 0.04 mM 1NA-PP1, and viewed under a Zeiss Axiophot microscope equipped with appropriate Zeiss filters for green fluorescent protein (GFP) and FM4-64 fluorescence.

2.3. Generation of the prk1-as3 allele

A *PRK1* fragment (nucleotide 302–1222) encoding the M108G mutation was amplified with the Taq polymerase (Roche) from genomic DNA using the oligonucleotides Nde,PRK1,mut (5′-CAACCA-TATGAGGTGTTTGTGTTAGGTGAATTTTGTGAACG-3′) and 3′Spe,PRK1 (5′-CATCAGAAAGTGGAACG-3′) and subcloned into pGEMT-easy by *Nde*I/*Spe*I. Next, the C175A mutation was introduced using the GeneEditor^{TM} in vitro site-directed mutagenesis system (Promega) and the primer 5′prk1C175A (5′-TGGCTTGTAC-AAAGTTGCTGATTTTGGTTCC-3′), generating pPRK1-M108G/

C175A. Another *PRK1* fragment encoding nucleotide −441 to 340, amplified by PCR, was subcloned into pPRK1-M108G/C175A via *Sac*I/*Nde*I restriction sites. The combined *Sac*I/*Spe*I PRK1-M108G/C175A fragment was subcloned into pRS316, opened with *Spe*I/*Sal*I and a third *PRK1 Spe*I/*Sal*I fragment encoding nucleotide 1151–2837, amplified by PCR, was inserted, generating pRS316-prk1-as3. All PCR-amplified regions were sequenced to verify the mutations and to exclude the presence of PCR errors.

2.4. Isolation of clathrin-coated vesicles

The procedure was performed according to [15], starting with 10 g (wet weight) of CB42 cells. The $100\,000 \times g$ pellet was homogenized in 1 ml of isolation buffer and centrifuged for 1 min at 13 000 rpm in a microcentrifuge. The supernatant was separated on a Sephacryl S-1000 column (80 cm long, 10 mm wide). Twenty five 4 ml fractions were collected, of which fractions #6 to #19 were analyzed by SDS–PAGE and immunoblotting using antibodies against Chc1p (S. Lemmon), PGK (Molecular Probes), actin (Roche), HA (Covance), Myc (Oncogene), and [^{125}I] Protein A. Quantitation of immunoreactive bands was performed with the phosphorimager (Molecular Dynamics).

For electron microscopy fractions #10 to #13 were fixed overnight in the presence of 2.5% (wt/vol) glutaraldehyde. After adsorption to freshly glow-discharged grids coated with a carbon support film, the mounted samples were washed with water and negatively stained with 2% aqueous uranyl acetate. Micrographs were taken at a primary magnification of 52 000× in a Philips CM 10 transmission electron microscope.

2.5. Affinity chromatography with glutathione S-transferase fusion proteins

Soluble glutathione *S*-transferase (GST), GST-Ypt7, and GST-Sjl2$_{890-1183}$ were purified according to the manufacturer's instructions. To prepare the yeast cell lysate, $1.75–2 \times 10^{10}$ cells (CB84) were converted to spheroplasts in 50 ml of 10 mM Tris/HCl (pH 7.5), 0.8 M sorbitol, 1 mM DTT, 0.5 mM PMSF, and 0.01 mg/ml Zymolyase 100T. Spheroplasts were lysed by dounce homogenization in 7 ml ice-cold lysis buffer (20 mM Hepes/KOH [pH 7.2], 0.1 M KCl, 2 mM MgCl2, 0.2 M sorbitol, 0.6% (wt/vol) Triton X-100, 1 mM DTT) containing protease inhibitors (0.5 mM PMSF, chymostatin, leupeptin, antipain, and pepstatin [each 5 μg/ml]). The lysate was centrifuged at $22\,000 \times g$ for 30 min and one milliliter of the supernatant was incubated with 40 μl bed volume of glutathione–Sepharose 4B preloaded with 80 μg of GST or GST-fusion proteins at 0 °C for 1 h. After washing the beads four times ($200 \times g$, 2 min) with lysis buffer, bound pro-

teins were eluted by three consecutive incubations with 250 μl of 20 mM reduced glutathione, 100 mM Tris/HCl (pH 9.0), 0.2 M NaCl, 5 mM DTT, 0.1% Triton X-100. Proteins were TCA-precipitated from the pooled eluates and analyzed by SDS–PAGE, Coomassie brilliant blue staining, and immunoblotting with α-Chc1p antibodies.

3. Results

3.1. Sjl2p localizes to punctate structures, which fully collapse in a mutant devoid of the actin-regulating kinases Ark1p and Prk1p

To address the question where in the cell Sjl2p functions, we analyzed its subcellular localization by indirect immunofluorescence and cell fractionation. We followed epitope-tagged versions of Sjl2p that either carried three copies of the hemagglutinin (HA), 13 copies of the c-Myc epitope, or the GFP at the C-terminus. These functional Sjl2p proteins were expressed from the chromosomal locus at wild-type levels (see Section 2).

Staining of HA-Sjl2p by indirect immunofluorescence revealed small punctate structures that were clearly visible above the background distributed evenly throughout the cell (Fig. 1A). These dots were not derived from endosomes or the Golgi complex, since they did not colocalize with endosomal marker proteins (Wicky and Singer-Krüger, unpublished) and did not collapse into large clusters in a vps27 (not shown) and a sec7 (Fig. 1A) mutant, in which a reorganization of endosomal and Golgi proteins has been demonstrated in various cases [16,17]. Furthermore, a concentration of HA-Sjl2p within a defined subcellular region, like sites of active growth, was not readily obvious. This finding was a bit surprising, since Bsp1p, a recently identified Sjl2p-binding protein, was found to colocalize with cortical patches [18], but may be explained by lower expression levels of Sjl2p. The colocalization of Bsp1p with actin scaffolds was most apparent in the Δark1Δprk1 mutant [19], in which the HA-Bsp1p staining pattern collapsed into large cytoplasmic clumps that contained actin and further cortical patch components [18]. The Ark1p/Prk1p kinases are members of a new family of serine/threonine kinases implicated in the regulation of critical components of the endocytic network [20]. When we studied the localization of HA-Sjl2p in Δark1 Δprk1 cells, we in fact observed a dramatic collapsing of the Sjl2p-positive structures generally into one or few large aggregate(s) per cell (Fig. 1B). Double label immunofluorescence revealed that the Sjl2p containing clumps were positive for actin (Fig. 2C) and Abp1p (not shown), an actin-binding protein intimately associated with cortical actin. Hence, in the Δark1 Δprk1 mutant we could indeed demonstrate a localization of Sjl2p to cortical actin patches.

To exclude the possibility that the loss of ARK1 and PRK1 indirectly affects the localization of Sjl2p, we made use of a mutant allele of PRK1, prk1-as3, a drug-sensitized kinase target, which can be specifically and almost instantaneously inactivated by a chemically-modified kinase inhibitor [21,22]. Mutant Δark1 prk1-as3 cells were incubated with this cell permeable inhibitor 4-amino-1-tert-butyl-3-(1′-naphthyl)pyrazolo[3,4-d]pyrimidine [21] for 2, 5, and 20 min to specifically inactivate Prk1-as3p and subsequently fixed and processed for indirect immunofluorescence. While in DMSO mock-treated cells the typical faint punctate HA-Sjl2p staining pattern was not affected (Fig. 1D, 0 min), incubation with the PP1-analog immediately led to a striking aggregation of Sjl2p with-
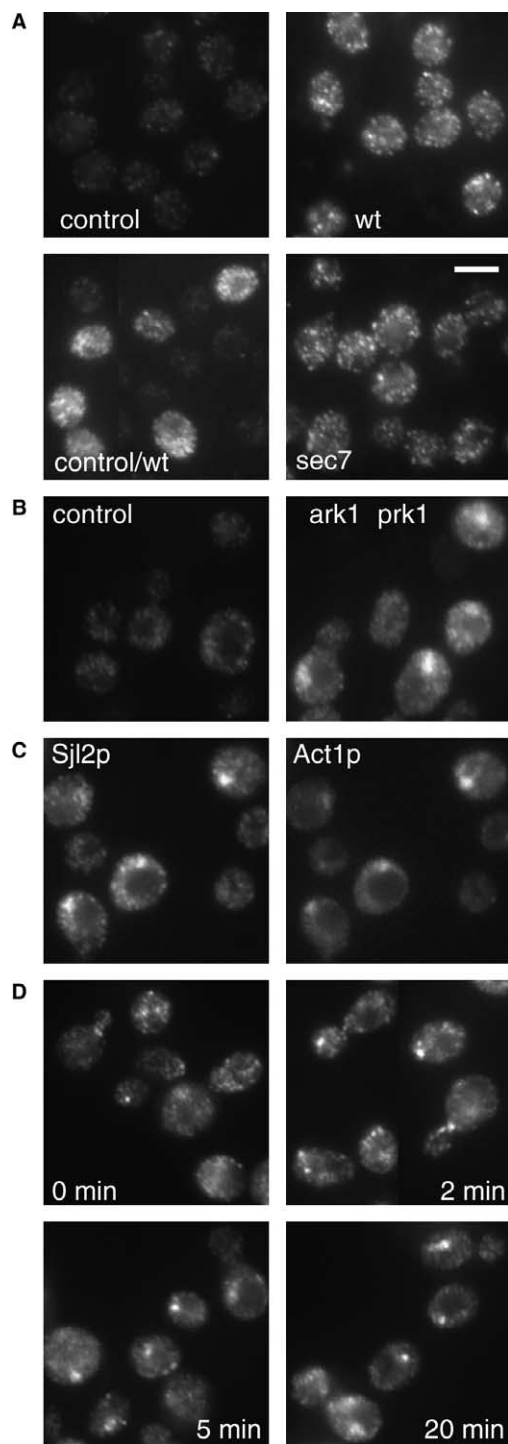

Fig. 1. Sjl2p colocalizes with actin clumps upon inactivation of the Ark1p/Prk1p kinases. (A) Untagged cells (BS64, control), cells expressing HA-Sjl2p in a wild-type (BS1128, wt) and sec7 (BS1175) background, and a mixture of untagged and wild-type epitope-tagged cells were stained with an anti-HA antibody; sec7 cells were fixed after a 2 h shift to 37 °C in medium containing 0.1% glucose; bar, 5 μm. (B) Untagged Δark1 Δprk1 cells (DDY1885) and Δark1 Δprk1 cells expressing HA-Sjl2p (BS1271) were stained with an anti-HA antibody. (C) BS1271 cells expressing GFP-Act1p were stained for HA-Sjl2p using an Alexa[594]-conjugate as secondary antibody. GFP-Act1p was detected by autofluorescence. (D) Δark1 prk1-as3 cells expressing HA-Sjl2p (BS1417) were incubated with 1NA-PP1 as indicated, fixed, and processed for indirect immunofluorescence as described in (A).
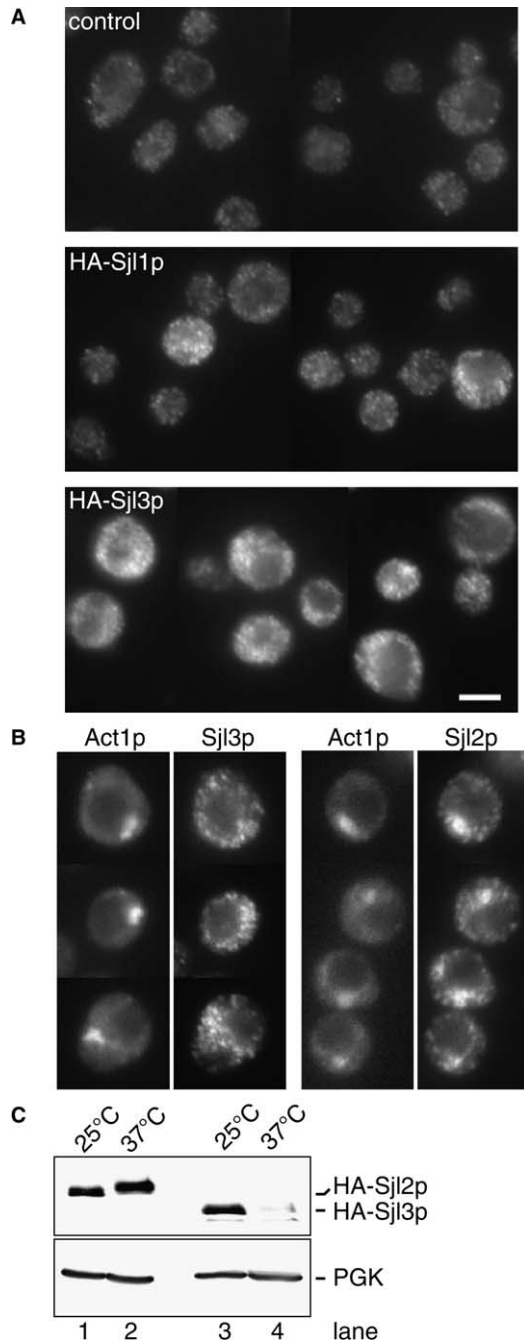
Fig. 2. Sjl1p and Sjl3p do not aggregate and colocalize with actin clumps upon inactivation of Ark1p/Prk1p. (A) Untagged Δark1 Δprk1 cells (DDY1885) and Δark1 Δprk1 cells expressing either HA-Sjl1p (BS1373) or HA-Sjl3p (BS1376) were stained with an anti-HA antibody; bar, 5 μm. (B) Transformants of BS1271 and BS1376 cells expressing GFP-Act1p were stained for HA-Sjl2p or HA-Sjl3p and GFP-Act1p as described in Fig. 1C. (C) Temperature-sensitive sec7 cells expressing either HA-Sjl2p (BS1175, lanes 1 and 2) or HA-Sjl3p (CB175, lanes 3 and 4) were harvested after growth at 25 °C and after a 2 h incubation at 37 °C in medium containing 0.1% glucose. Samples were processed for immunoblotting with an anti-HA and an anti-PGK antiserum.

in the cell. After 2 min, the Sjl2p-positive aggregates were frequently present within the buds and bud-necks of small budded cells and after 5–20 min, they were found usually in the mother cells (Fig. 1D).

3.2. Sjl1p and Sjl3p do not respond to Ark1p/Prk1p inhibition and likely act at distinct subcellular locations

Remarkably, the incorporation of Sjl2p into large actin clumps was unique among the three synaptojanin-like proteins. In cells lacking PRK1 and ARK1 the staining pattern of HA-Sjl1p, which was hardly detectable over background [11], did not collapse into clumps and the slightly stronger punctate and diffuse cytoplasmic HA-Sjl3p staining was also unaffected (Fig. 2A). The absent response to Ark1p/Prk1p inhibition was also confirmed by treatment with 1NA-PP1 in Δark1 prk1-as3 cells expressing HA-Sjl3p (data not shown). Most significantly, double staining of GFP-Act1p and HA-Sjl1p or of HA-Sjl3p after 20 min of inhibitor treatment did not reveal an overlap between cortical actin and Sjl1p (not shown) or Sjl3p, respectively (Fig. 2B). This is in sharp contrast to Sjl2p, whose staining pattern perfectly matched that of actin (Figs. 2B and 1C). The specific response of Sjl2p to Prk1p-inactivation is the first biochemical evidence for an individual and discrete subcellular role of Sjl2p in the context of the two other synaptojanin family members.

Further support for distinct subcellular localizations and features of Sjl2p and Sjl3p was provided by analyzing the effect of the sec7 mutation on the localization and stability of HA-Sjl3p. While in the sec7 mutant after shift to 37 °C the HA-Sjl2p staining pattern was similar to wild-type (Fig. 1A), the HA-Sjl3p signal was lost after shift to 37 °C (data not shown). This result was confirmed by immunoblotting of cell extracts prepared from sec7 cells after incubation at 25 and 37 °C. Whereas the amounts of HA-Sjl2p were comparable under both conditions, the levels of HA-Sjl3p were strongly reduced after incubation at restrictive temperature (Fig. 2C). Although the basis for this effect is presently not understood, the defect in the biogenesis of phospholipids may result in the dissociation of the lipid phosphatase from the membrane and subsequent degradation, consistent with a function of HA-Sjl3p at the late Golgi, where an improper lipid and protein composition likely becomes evident first. Another interesting observation was that the apparent molecular weight of HA-Sjl2p slightly increased after incubation at restrictive conditions in sec7 cells (Fig. 2C). We are currently investigating the nature of this alteration.

3.3. Sjl2p overlaps with structures containing endocytosed FM4-64

To provide evidence for a shared role of Sjl2p within the cortical actin cytoskeleton and in endocytosis as previously proposed [7,8,18,23], we analyzed whether FM4-64, a fluorescent membrane marker for endocytosis, colocalized with GFP-Sjl2p after drug inhibition of Prk1-as3p. Cells were allowed to bind FM4-64 at 0 °C, washed with ice-cold medium to remove unbound dye, and incubated at 25 °C for 10 min in the absence and presence of 1NA-PP1. Subsequently, endocytosis was terminated by the addition of energy poisons. While in the absence of 1NA-PP1 no overlap between the endosomal FM4-64 labeling and GFP-Sjl2p was detected (likely due to the low GFP-Sjl2p signal in small punctate structures), treatment with 1NA-PP1 affected the collapsing of both the GFP-Sjl2p- and a fraction of the FM4-64-positive structures (Fig. 3A). The overlap of those structures (Fig. 3A) clearly suggests that the aggregates containing Sjl2p, actin, and other cortical patch components also enclose endocytic membranes. This is consistent with the previous observation that vesicles
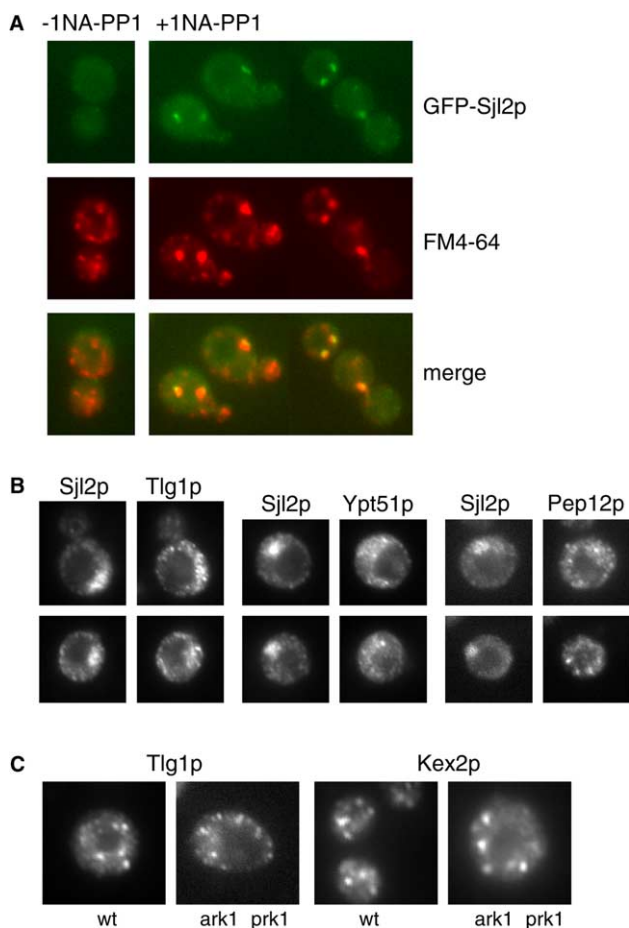
Fig. 3. The Sjl2p- and actin-containing clusters colocalize with endocytosed FM4-64, but not with endosomal or TGN-derived structures. (A) Δ*ark1 prk1-as3* cells expressing GFP-Sjl2p (BS1446) were labeled with FM4-64 as described. Cells were photographed with appropriate filters for GFP and FM4-64 fluorescence; bar, 5 μm. (B) Fixed cells (BS1271) were first stained with an anti-HA antibody to label HA-Sjl2p and second with either α-Pep12p, α-Ypt51p, or α-Myc antibodies. (C) Wild-type (BS64) and Δ*ark1* Δ*prk1* (DDY1885) cells expressing Myc-Tlg1p or HA-Kex2p were stained with an anti-Myc or anti-HA antibody, respectively.

of likely endocytic origin accumulate within the actin clumps of inhibitor-treated Δ*ark1 prk1-as3* cells [22]. The additional FM4-64 positive structures that did not cluster and colocalize with Sjl2p upon inhibitor treatment likely represent more distally located endocytic compartments (see below).

3.4. Sjl2p-positive clumps do not overlap with endosomes and the TGN and are formed regardless of Sec18p/NSF

To elucidate what sort of endocytic structures colocalize with the Sjl2p-containing actin clumps, we performed double immunofluorescence. Consistent with the lack of colocalization of HA-Sjl2p with the early and late endosomal markers Tlg1p, Ypt51p, and Pep12p in wild-type and *vps27* cells (see above), in inhibitor-treated Δ*ark1 prk1-as3* cells the staining patterns of Sjl2p and each of the three endosomal markers did not largely overlap (Fig. 3B). Although Tlg1p, a marker of recycling endosomes and the TGN, was usually found in close proximity of the Sjl2p clumps, it did not aggregate itself upon 1NA-PP1 treatment, but rather localized to smaller dots dispersed in a larger region of the cell (Fig. 3C). This was also

the case for Ypt51p, Pep12p (data not shown) and a marker of the TGN, Kex2p (Fig. 3C). Hence, as opposed to the aggregation of FM4-64 containing vesicles Ark1p/Prk1p inhibition does not affect the subcellular organization of endosomes and the TGN.

Since the data suggested that the Sjl2p-positive endosomal structures may represent primary endocytic vesicles, we assumed that inactivation of Sec18p/*N*-ethylmaleimide-sensitive fusion protein (NSF), a cytoplasmic AAA$^+$-ATPase required for most intracellular membrane fusion events including an early postinternalization step within the endocytic pathway [24], would not affect clump formation. We introduced the temperature-sensitive *sec18–20* allele into the Δ*ark1 prk1-as3* strain background. Sec18p encoded by this allele is active at 25 °C but is inactivated immediately upon shift to 32 °C [24]. Indeed, FM4-64 internalization and FM4-64 and GFP-Sjl2p clump formation occured at 25 and 32 °C regardless of the activity of Sec18p (data not shown). Thus, the endosomal structures that cluster upon loss of the Ark1p/Prk1p kinases likely represent nascent endocytic vesicles derived from the plasma membrane after budding.

3.5. The Synaptojanin-like proteins display distinct elution profiles from a Sephacryl S-1000 gel filtration column

Since in yeast biochemical evidence for an association of any of the synaptojanin-like 5′-phosphatases with vesicular structures is still lacking, we isolated clathrin-coated vesicles from a yeast strain carrying epitope-tagged versions of Sjl1p, Sjl2p, and Sjl3p, thus allowing the simultaneous detection of each synaptojanin-like protein in one and the same cell extract. Similar to Chc1p, each synaptojanin-like protein was enriched in a $100000 \times g$ microsomal pellet, obtained after hypotonic lysis of spheroplasts (Fig. 4A). However, gel filtration chromatography of the homogenized P100 fraction on a Sephacryl S-1000 column revealed clear differences among Sjl1p, Sjl2p, and Sjl3p. While Sjl2p and Sjl3p eluted from the column very similar to Chc1p (Fig. 4B), the Sjl1p peak was clearly separated from Chc1p, but corresponded to the profiles of cytosolic PGK and actin (not shown), peaking in fraction #15. Unlike Sjl3p, the Sjl2p elution profile contained a typical shoulder (Fig. 4B). The amounts of Sjl2p in fractions #14 and #15 following the major Sjl2p-peak could represent a soluble pool that dissociated from membranes during the preparation. The specific elution profiles of the individual synaptojanin-like proteins, Chc1p, and other marker proteins were highly reproducible and indicated a differential localization of Sjl2p/Sjl3p and Sjl1p to membrane vesicles or the cytoplasm, respectively.

Analysis of the Sephacryl S-1000 column fractions by electron microscopy after negative staining confirmed the presence and high enrichment of authentic clathrin-coated vesicles in addition to uncoated vesicles (Fig. 4C). A quantitative analysis revealed that the proportion of clathrin-coated structures (average diameter 64 ± 7 nm) was highest in fraction #10 (87%, $n = 175$) and #11 (56%, $n = 177$). Fraction #12 was largely composed of smooth membrane vesicles (83%, $n = 138$) with an average diameter of 38 ± 3 nm (Fig. 4B). Finally, some of the few vesicular structures found in fraction #13 contained coats that appeared more dense than those of authentic clathrin-coated vesicles (Fig. 4C). In fraction #13, we also observed the high enrichment of a symmetric protein structure, most likely fatty acid synthase [25] (Fig. 4C).
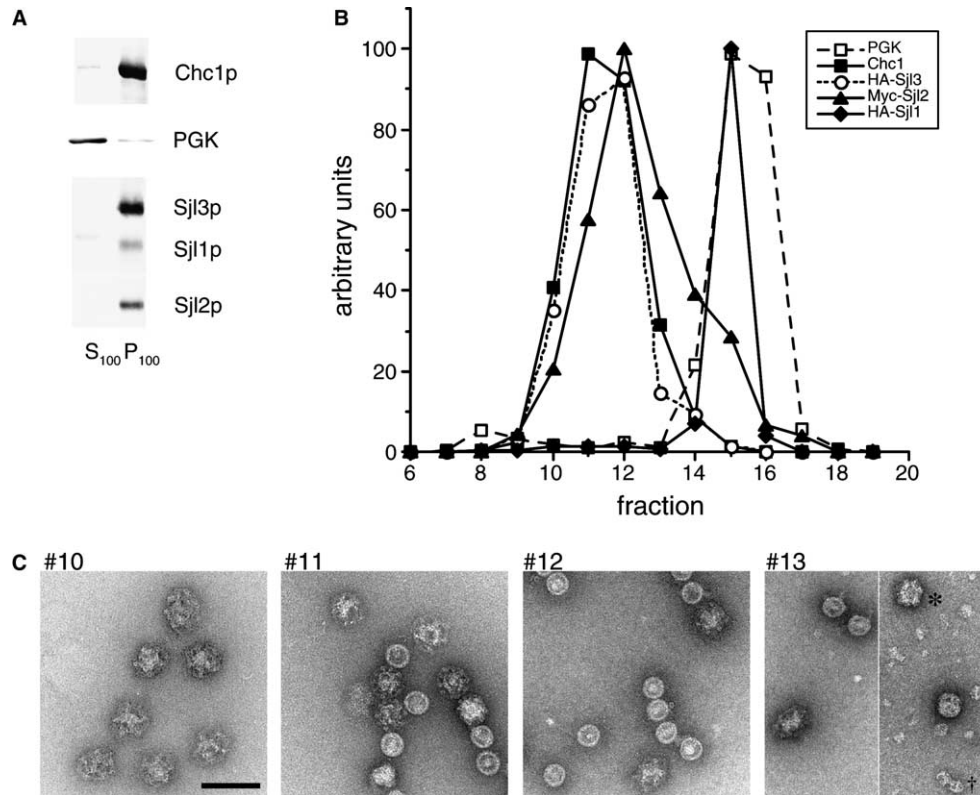
Fig. 4. Sjl2p and Sjl3p fractionate similar to clathrin-coated vesicles, while Sjl1p does not. (A) A precleared lysate of cells (CB42) was centrifuged at $100\,000 \times g$ to generate the pellet and supernatant fractions P_{100} and S_{100}. Equal protein amounts were analyzed by immunoblotting with antibodies against the HA- and the Myc-epitope, Chc1p, and PGK. (B) The P_{100} fraction was fractionated by Sephacryl S-1000 gel filtration chromatography. Fractions #6 to #19 were analyzed by immunoblotting as described. The immunoreactive bands were quantified with the phosphorimager. The isolation was performed seven times, shown is one representative experiment. (C) Fractions #10 to #13 were fixed with 2.5% glutaraldehyde. After negative staining, samples were viewed in the electron microscope at a magnification of 52 000; bar, 100 nm; [*], densely coated vesicle; [†], fatty acid synthase particle.

Unfortunately, so far we could not detect Sjl2p and Sjl3p on the vesicular structures by immuno EM. It appears however, that Sjl2p and Sjl3p reside on clathrin-coated and/or non-coated vesicular structures with a diameter close to that of clathrin-coated vesicles. This would be consistent with a role of the lipid phosphatases Sjl2p and Sjl3p, but not Sjl1p, in the uncoating of yeast clathrin-coated vesicles.

3.6. Inclusion of clathrin in the Sjl2p-containing actin clumps

To provide further independent evidence for the idea that Sjl2p-positive vesicles are derived from clathrin-coated structures, we analyzed the cellular distribution of clathrin in wild-type and Δark1 prk1-as3 cells. Since the Sjl3p-containing vesicles, which are likely TGN-derived [26], do not aggregate in response to Prk1-as3 inhibition (Fig. 2A/B), clathrin-containing clumps induced by Prk1-as3 inactivation likely contain Sjl2p, cortical patch components, and early endocytic vesicles.

By indirect immunofluorescence, we labeled functional clathrin light chain (Clc1p) tagged N-terminally with an HA-epitope. As expected for an association with TGN- and plasma membrane-derived vesicles, in wild type HA-Clc1p was found in punctate structures (Fig. 5A). The weak cytoplasmic staining probably reflects the presence of Clc1p in non-assembled triskelions (Fig. 5A). In prk1-as3 cells, in the absence of 1NA-PP1, the Clc1p staining pattern was comparable to that in wild type (Fig. 5A). In contrast, treatment with 1NA-PP1 resulted in the instantaneous clustering of clathrin structures.

After 5 min of drug administration, usually one to two large Clc1p-aggregates per cell were observed in addition to smaller structures that did not cluster (Fig. 5A). Double staining of 13-Myc-Sjl2p and HA-Clc1p in Δark1 prk1-as3 cells after 10 min of drug treatment revealed a colocalization of both proteins in the clumps (Fig. 5B). Since clathrin is also implicated in membrane trafficking from the TGN, a structure unaffected by Ark1p/Prk1p inhibition, a lack of complete colocalization between Clc1p and Sjl2p is in fact not surprising.

3.7. Physical interaction between the proline-rich domain of Sjl2p and Chc1p

Because the proline-rich domain of Sjl2p contains the sequence LIDLD that matches the L(L/I)(D/E/N)(L/F)(D/E) consensus motif for binding to the terminal domain of clathrin heavy chain [27], we tested whether the Sjl2p proline-rich domain can bind to Chc1p. A glutathione S-transferase (GST) fusion containing amino acids 890–1183 (GST-Sjl2$_{890-1183}$) was expressed in Escherichia coli and purified by glutathione–Sepharose affinity purification. Similarly, GST alone and a GST-Ypt7p fusion were purified to serve as negative controls during the subsequent binding studies. GST and GST-fusions were immobilized on glutathione–Sepharose beads and incubated with a yeast cell lysate. We detected specific binding of Chc1p to GST-Sjl2$_{890-1183}$ but no binding to the control recombinant proteins (Fig. 5C). Thus, Sjl2p can bind to clathrin in vitro.
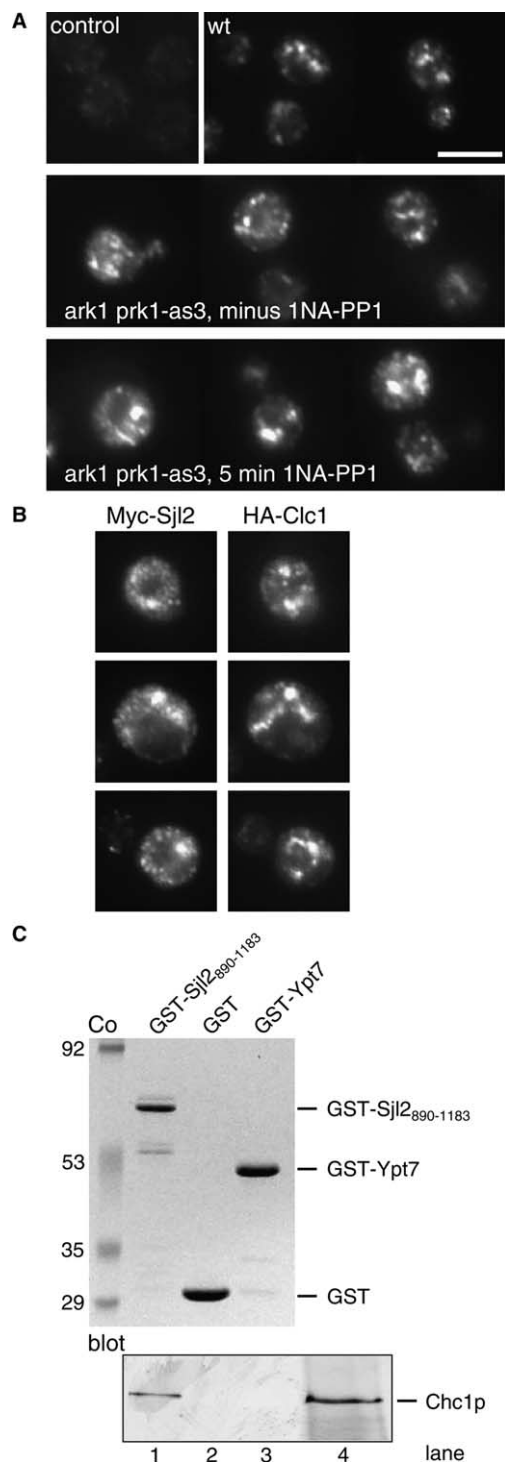
Fig. 5. Clathrin aggregates immediately after Prk1-as3p inactivation and interacts with Sjl2p in vitro. (A) Untagged cells (BS64) and *ARK1 PRK1* cells expressing HA-Clc1p (BS1516, wt) were stained with an anti-HA antibody. Similarly, Δ*ark1 prk1-as3* cells expressing HA-Clc1p cells were incubated with DMSO (minus 1NA-PP1) or 1NA-PP1, fixed and stained as described above; bar, 5 μm. (B) Double indirect immunofluorescence with Δ*ark1 prk1-as3* cells expressing HA-Clc1p and Myc-Sjl2p (BS1569) incubated with 1NA-PP1 for 10 min. (C) GST and GST-fusions were immobilized onto glutathione–Sepharose beads and incubated with a yeast cell lysate. After extensive washing, bound proteins were eluted and separated by SDS–PAGE. Recombinant proteins were stained with Coomassie brilliant blue (Co), Chc1p was detected by immunoblotting. The input lane 4 represents 3% of the cell lysate that was incubated with each immobilized protein.

In a reverse GST pull-down experiment in which the terminal domain of Chc1p (GST-Chc1p$_{1-369}$) was incubated with an extract containing Myc-Sjl2p, no interaction was observed between the two proteins (data not shown). This may either reflect a deficiency in the proper folding of the β-propeller domain. Conversely, the association of Chc1p with the proline-rich domain of Sjl2p may be mediated or stabilized by additional regions within the clathrin molecule.

4. Discussion

4.1. Sjl2p specifically functions within the early endocytic pathway

The two partially redundant kinases, Prk1p and Ark1p, have emerged as excellent candidates that control the timing and level of endocytic actin polymerization. They were recently suggested to act in the transition from vesicle formation to targeting and fusion via Pan1p [28], one of the three yeast Arp2/3p activators. Because members of the conserved Ark1p/Prk1p kinases specifically control endocytic membrane trafficking in all eukaryotes [20], the specific and immediate response of Sjl2p to Ark1p/Prk1p inhibition and the colocalization of Sjl2p with the endosomal tracer FM4-64 and cortical actin strongly support a major role of Sjl2p during endocytosis. The Sjl2p-positive structures isolated by subcellular fractionation most likely represent, or are derived from, clathrin-coated vesicles generated after budding from the plasma membrane. Firstly, Sjl2p is largely membrane-associated (Böttcher and Singer-Krüger, unpublished results) and fractionates very similar to clathrin-coated vesicles. Secondly, a fraction of clathrin is also sensitive to Ark1p/Prk1p inhibition and colocalizes with Sjl2p. Thus, it likely represents the endocytic pool. Neither TGN-localized Sjl3p nor Kex2p, which are functionally connected to clathrin [10,26], aggregate upon loss of Ark1p/Prk1p activity. Thirdly, a physical interaction was identified between the proline-rich domain of Sjl2p and Chc1p which in part may be mediated by a conserved clathrin binding box. In summary, Sjl2p appears to reside mainly on plasma membrane-derived primary clathrin-coated and/or uncoated endocytic vesicles that are generated prior to the activity of Sec18p/NSF during endocytosis. If any, only minor quantities of Sjl2p localize to the plasma membrane and/or endosomes. It will be important to determine the precise regulation of Sjl2p's enzymatic activity during endocytic vesicle maturation and the sequence of interactions with cytoskeletal elements, the vesicle membrane, coat and adaptor components during this process.

4.2. Physical linkage of the synaptojanin-like proteins to cortical actin and to clathrin

Evidence for a physical link between the yeast synaptojanin-like proteins and cortical actin was initially provided by studies in which GFP-tagged PPIP- and proline-rich domains of Sjl2p and Sjl3p were overexpressed and their transient colocalization with actin patches observed under conditions of hyperosmotic stress [29]. Subsequently, two-hybrid and biochemical studies led to the identification of Bsp1p and Abp1p as binding partners of Sjl2p/Sjl3p [18,23]. Furthermore, the staining pattern of Sjl2p-GFP was recently found to overlap with actin patches [24], similar to the colocalization of Sjl2p with actin clumps in *ark1 prk1* cells shown here. Taking advantage of the possibility to detect endogenous levels of each synaptojanin-like

protein in one and the same cell extract, we could demonstrate the association of Sjl1p, Sjl2p, and Sjl3p with actin polymerized in vitro (Böttcher and Singer-Krüger, unpublished results) using an established biochemical assay [30]. Yet, despite this common feature of the yeast Synaptojanin-like proteins, loss of the Ark1p/Prk1p kinases mainly affects the subcellular distribution of Sjl2p. Conversely, in a *sec7* mutant which accumulates Golgi stacks and is impaired in the biogenesis of TGN proteins and lipids the localization and stability of Sjl3p, but not Sjl2p, was found to be affected lending further support of the idea of distinct subcellular localizations of these synaptojanin family members. Similar to our finding of a colocalization of clathrin and Sjl2p within cortical actin patches, the association of clathrin with cortical actin was demonstrated by recent work of Lemmon and coworkers [31]. It is interesting that Sjl2p and Sjl3p bind to clathrin heavy chain (this work and [26]), likely via the conserved L(L/I)(D/E/N)(L/F)(D/E) motif, and migrate similar to clathrin-coated vesicles, while in the case of Sjl1p no evidence for a colocalization with clathrin exists until now. In conclusion, our studies corroborate the functional connection between some yeast synaptojanin family members and clathrin as has been originally proposed by the phenotypic characterization of the synaptojanin 1 knock-out mouse [32]. This work also revealed distinct features of the three yeast synaptojanin-like proteins. Future studies will likely shed more light on the exact roles of synaptojanin and clathrin during the process of clathrin-uncoating.

References

[1] Roth, M.G. (2004) Phosphoinositides in constitutive membrane traffic. Physiol. Rev. 84, 699–730.
[2] Harris, T.W., Hartwieg, E., Horvitz, H.R. and Jorgensen, E.M. (2000) Mutations in synaptojanin disrupt synaptic vesicle recycling. J. Cell Biol. 150, 589–600.
[3] Kim, W.T., Chang, S., Daniell, L., Cremona, O., Di Paolo, G. and De Camilli, P. (2002) Delayed reentry of recycling vesicles into the fusion-competent synaptic vesicle pool in synaptojanin 1 knockout mice. Proc. Natl. Acad. Sci. USA 99, 17143–17148.
[4] Verstreken, P., Koh, T.W., Schulze, K.L., Zhai, R.G., Hiesinger, P.R., Zhou, Y., Mehta, S.Q., Cao, Y., Roos, J. and Bellen, H.J. (2003) Synaptojanin is recruited by endophilin to promote synaptic vesicle uncoating. Neuron 40, 733–748.
[5] Srinivasan, S., Seaman, M.N., Nemoto, Y., Daniell, L., Suchy, S.F., Emr, S.D., De Camilli, P. and Nussbaum, R. (1997) Disruption of three phosphatidylinositol-polyphosphate 5-phosphatase genes from *Saccharomyces cerevisiae* result in pleiotropic abnormalities of vacuole morphology, cell shape, and osmohomeostasis. Eur. J. Cell Biol. 74, 350–360.
[6] Stolz, L.E., Huynh, C.V., Thorner, J. and York, J.D. (1998) Identification and characterization of an essential family of inositol polyphosphate 5-phosphatases (INP51, INP52, and INP53 gene products) in the yeast *Saccharomyces cerevisiae*. Genetics 148, 1715–1729.
[7] Singer-Krüger, B., Nemoto, Y., Daniell, L., Ferro-Novick, S. and De Camilli, P. (1998) Synaptojanin family members are implicated in endocytic membrane traffic in yeast. J. Cell Sci. 111, 3347–3356.
[8] Stefan, C.J., Audhya, A. and Emr, S.D. (2002) The yeast synaptojanin-like proteins control the cellular distribution of phosphatidylinositol (4,5)-bisphosphate. Mol. Biol. Cell 13, 542–557.
[9] Wendland, B. and Emr, S.D. (1998) Pan1, yeast eps15, functions as a multivalent adaptor that coordinates protein–protein interactions essential for endocytosis. J. Cell Biol. 141, 71–84.
[10] Bensen, E.S., Costaguta, G. and Payne, G.S. (2000) Synthetic genetic interactions with temperature-sensitive clathrin in *Saccharomyces cerevisiae*. Roles for synaptojanin-like Inp53p and dynamin-related Vps1p in clathrin-dependent protein sorting at the *trans*-Golgi network. Genetics 154, 83–97.
[11] Morales-Johansson, H., Jenoe, P., Cooke, F.T. and Hall, M.N. (2004) Negative regulation of phosphatidylinositol 4,5-bisphosphate levels by the INP51-associated proteins TAX4 and IRS4. J. Biol. Chem. 279, 39604–39610.
[12] Longtine, M.S., McKenzie, A., Demarini, D.J., Shah, N.G., Wach, A., Brachat, A., Philippsen, P. and Pringle, J.R. (1998) Additional modules for versatile and economical PCR-based gene deletion and modification in *Saccharomyces cerevisiae*. Yeast 14, 953–961.
[13] Wicky, S., Schwarz, H. and Singer-Krüger, B. (2004) Molecular interactions of yeast Neo1p, an essential member of the Drs2 family of aminophospholipid translocases, and its role in membrane trafficking within the endomembrane system. Mol. Cell. Biol. 24, 7402–7418.
[14] Jochum, A., Jackson, D., Schwarz, H., Pipkorn, R. and Singer-Krüger, B. (2002) Yeast Ysl2p, homologous to Sec7 domain guanine nucleotide exchange factors, functions in endocytosis and maintenance of vacuole integrity and interacts with the Arf-like small GTPase Arl1p. Mol. Cell. Biol. 22, 4914–4928.
[15] Mueller, S.C. and Branton, D. (1984) Identification of coated vesicles in *Saccharomyces cerevisiae*. J. Cell Biol. 98, 341–346.
[16] Piper, R.C., Cooper, A.A., Yang, H. and Stevens, T.H. (1995) VPS27 controls vacuolar and endocytic traffic through a prevacuolar compartment in *Saccharomyces cerevisiae*. J. Cell Biol. 131, 603–617.
[17] Segev, N., Mulholland, J. and Botstein, D. (1988) The yeast GTP-binding YPT1 protein and a mammalian counterpart are associated with the secretory machinery. Cell 52, 915–924.
[18] Wicky, S., Frischmuth, S. and Singer-Krüger, B. (2003) Bsp1p/Ypr171p is an adapter that directly links some synaptojanin family members to the cortical actin cytoskeleton in yeast. FEBS Lett. 537, 35–41.
[19] Cope, M.J., Yang, S., Shang, C. and Drubin, D. (1999) Novel protein kinases Ark1p and Prk1p associate with and regulate the cortical actin cytoskeleton in budding yeast. J. Cell Biol. 144, 1203–1218.
[20] Smythe, E. and Ayscough, K.R. (2003) The Ark1/Prk1 family of protein kinases. Regulators of endocytosis and the actin skeleton. EMBO Rep. 4, 246–251.
[21] Bishop, A.C., Shah, K., Liu, Y., Witucki, L., Kung, C. and Shokat, K.M. (1998) Design of allele-specific inhibitors to probe protein kinase signaling. Curr. Biol. 8, 257–266.
[22] Sekiya-Kawasaki, M., Groen, A.C., Cope, M.J., Kaksonen, M., Watson, H.A., Zhang, C., Shokat, K.M., Wendland, B., McDonald, K.L., McCaffery, J.M. and Drubin, D.G. (2003) Dynamic phosphoregulation of the cortical actin cytoskeleton and endocytic machinery revealed by real-time chemical genetic analysis. J. Cell Biol. 162, 765–772.
[23] Stefan, C.J., Padilla, S.M., Audhya, A. and Emr, S.D. (2005) The phosphoinositide phosphatase Sjl2 is recruited to cortical actin patches in the control of vesicle formation and fission during endocytosis. Mol. Cell. Biol. 25, 2910–2923.
[24] Hicke, L., Zanolari, B., Pypaert, M., Rohrer, J. and Riezman, H. (1997) Transport through the yeast endocytic pathway occurs through morphologically distinct compartments and requires an active secretory pathway and Sec18p/N-ethylmalemidesensitive fusion protein. Mol. Biol. Cell 8, 13–31.
[25] Kolodziej, S.J., Penczek, P.A., Schroeter, J.P. and Stoops, J.K. (1996) Structurefunction relationships of the *Saccharomyces cerevisiae* fatty acid synthase. J. Biol. Chem. 271, 28422–28429.
[26] Ha, S.A., Torabinejad, J., DeWald, D.B., Wenk, M.R., Lucast, L., De Camilli, P., Newitt, R.A., Aebersold, R. and Nothwehr, S.F. (2003) The synaptojanin-like protein Inp53/Sjl3 functions with clathrin in a yeast TGN-to-endosome pathway distinct from

the GGA protein-dependent pathway. Mol. Biol. Cell 14, 1319–1333.

[27] Dell'Angelica, E.C., Klumperman, J., Stoorvogel, W. and Bonifacino, J.S. (1998) Association of the AP-3 adaptor complex with clathrin. Science 280, 431–434.

[28] Toshima, J., Toshima, J.Y., Martin, A.C. and Drubin, D.G. (2005) Phosphoregulation of Arp2/3-dependent actin assembly during receptor-mediated endocytosis. Nat. Cell Biol. 7, 246–254.

[29] Ooms, L.M., McColl, B.K., Wiradjaja, F., Wijayaratnam, A.P., Gleeson, P., Gething, M.J., Sambrook, J. and Mitchell, C.A. (2000) The yeast inositol polyphosphate 5-phosphatases Inp52p and Inp53p translocate to actin patches following hyperosmotic stress: mechanism for regulating phosphatidylinositol 4,5-bis-phosphate at plasma membrane invaginations. Mol. Cell. Biol. 20, 9376–9390.

[30] Goode, B.L. (2002) Purification of yeast actin and actin-associated proteins. Methods Enzymol. 351, 433–441.

[31] Newpher, T.M., Smith, R.P., Lemmon, V. and Lemmon, S.K. (2005) In vivo dynamics of clathrin and its adaptor-dependent recruitment to the actin-based endocytic machinery in yeast. Dev. Cell 9, 87–98.

[32] Cremona, O., Di Paolo, G., Wenk, M.R., Luthi, A., Kim, W.T., Takei, K., Daniell, L., Nemoto, Y., Shears, S.B., Flavell, R.A., McCormick, D.A. and De Camilli, P. (1999) Essential role of phosphoinositide metabolism in synaptic vesicle recycling. Cell 99, 179–188.